Equal-Distance Sampling of Superellipse Models

Maurizio Pilu **Robert B. Fisher**

Department of Artificial Intelligence
The University of Edinburgh
5 Forrest Hill, Edinburgh EH1 2QL
SCOTLAND

Abstract

Superellipses are parametric models that can be used for representing two dimensional object parts or aspects of 3-D parts. Previously little care was given to obtaining a precise sampling of the contour of these models. Equal-distance sampling of superellipse model contours is however important for rendering and in cases in which a cost function needs to be estimated for data fitting or parameter estimation, such as in model-based optimisation. In this paper we present a new parametric method for achieving equal-distance sampling of superellipse model contours that properly combines two simple first order models of the sampled points distance function. We also show how to extend the method to deformable superellipses and superquadrics.

1 Introduction

Superellipses and their 3-D extension superquadrics were invented by Hein [3] and brought to the computer graphics and vision community mainly by Barr [1] and Pentland [4]. They can represent many closed 2-D and 3-D shapes (e.g. [6, 5, 7, 4]) in a straightforward and natural way by using few parameters and moreover simple deformation can be applied to extend their modelling capabilities.

Pentland [5] and other leading vision researchers first introduced superquadrics as a model to coarsely represent parts of objects with a minimum description in the Huffmann coding sense (i.e. number of bits). Indeed one of the main advantages of superquadrics is their compactness of representation. As well as superquadrics, superellipses can be used to model aspects of parts of 3-D objects, as shown in Figure 1.

Superquadrics and superellipses, however, are mathematical objects of particularly awkward nature because they are the result of strong non-linearities caused by fractional exponents, which cannot be analytically easily dealt with.

In many works that use superquadrics, it can be noticed that superquadrics are not sampled in a regular way when rendering and computing cost or Error of Fit (EOF) functions (such as in [8]),

BMVC 1995 doi:10.5244/C.9.26

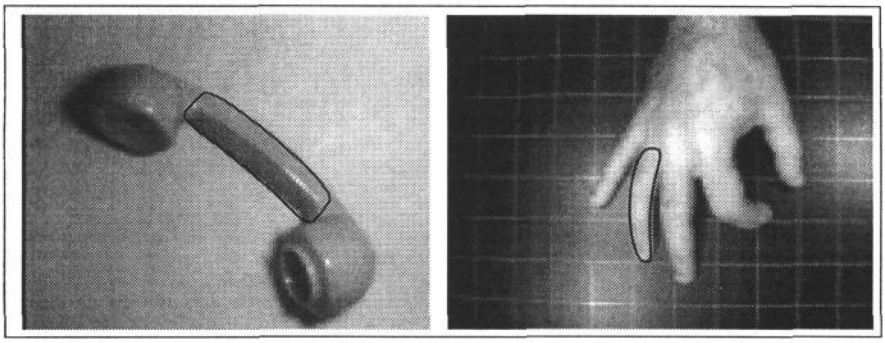

Figure 1: Two examples of modelling aspects of parts by deformable superellipses

In some applications, such as in *Model-based Optimisation*, we need to compute cost functions across superquadric surfaces or superellipse contours (either deformed or undeformed) and the irregular sampling causes some regions to have an higher weight on the final cost, evidently producing wrong results with real data.

Franklin and Barr [2] partially solved this problem by using an explicit non-parametric method. This greatly improved precision and speed but still has 20-30% error in the sampling distance and could not deal with sampling deformed superellipses. They were against parametric sampling because its complexity and slowness.

This paper presents a solution to the problem of providing a reasonably fast and reliable parametric method for obtaining a given constant sampling distance along the whole contour of arbitrary superellipses and we will also show how to extend the method to deformed models.

By using the spherical product [1] , the method can also be trivially extended to superquadrics.

2 Superellipses and Deformations

A superellipse can be described by the 2-D vector:

$$\mathbf{x}(\theta) = \begin{bmatrix} a_1 cos(\theta)^\epsilon \\ a_2 sin(\theta)^\epsilon \end{bmatrix} \tag{1}$$

$$-\pi \leq \theta \leq \pi$$

where a_1 and a_2 are the two semiaxis and $0 \leq \epsilon \leq 1$ is the roundness parameter. By eliminating θ, its implicit equation can be easily obtained:

$$\left(\frac{x}{a_1}\right)^{2/\epsilon} + \left(\frac{y}{a_2}\right)^{2/\epsilon} = 1 \tag{2}$$

Either simple or complicated deformations can be applied to the basic superellipses shapes. The two most common deformations are *linear tapering* and *circular bending* along the principal axis of the superellipse.

By simple geometric considerations (see, e.g., [8] for the details) and indicating by capital letters the coordinates of the transformed shape, a tapering deformation along the y-axis transforming a point $[x\ y]^T$ is defined as:

$$\begin{cases} X = f_x(y)x \\ Y = y \end{cases} \tag{3}$$

.

If $f_x(y)$ is linear the tapering will also be linear. By setting $f_x(y) = \frac{T_x}{a2}y + 1$, with $-1 \leq T_x \leq 1$, we have linear tapering ranging from increasing cross-section ($T_x > 0$), decreasing cross-section ($T_x < 0$) and constant section ($T_x = 0$).

In the same way, a circular bending deformation along the y-axis is given by

$$\begin{cases} X = x + sign(c) * (\sqrt{y^2 + r^2} - r) \\ Y = sin(\gamma) * r \end{cases} \tag{4}$$

where:

$$\begin{gathered} R = a_2/c \\ r = R - |x| \\ \gamma = atan(y/r) \end{gathered}$$

and $-1 \leq T_x \leq 1$ is the normalized bending parameter. A combination of deformations should be carried out by first doing the deformations that are more shape preserving (see e.g. [8]). In our case, with just two deformations used, the right order is tapering first and bending afterwards.

3 Linear Sampling and Explicit Method

In this section we show the result of sampling the model using plain linear increase of the θ parameter and the explicit method proposed by Franklin and Barr in [2].

In Figure 2 (top) we see a linearly sampling superellipse parameter and a graph expressing the distance of successive samples. It can be easily seen that this method, though fast and simple, can only have very limited applications: points are very evenly spaced and mostly gathered near the corners.

Figure 2 (bottom) shows instead the sampling proposed by Franklin and Barr in which one of the coordinates is assigned and the other is computed by solving equation 2 for the former. The outcome of this sampling is considerably better than one with the previous method but, as it can be seen from the graph of the distance, it still gives more than 30% error. (The spike is due to a mismatch between the two halves of the quadrant at the junction.) Moreover, this method rely on a straight approximation of the two sides of the superellipse quadrant and therefore cannot deal with any kind of deformation, which would only worsen the distance spread along the contour.

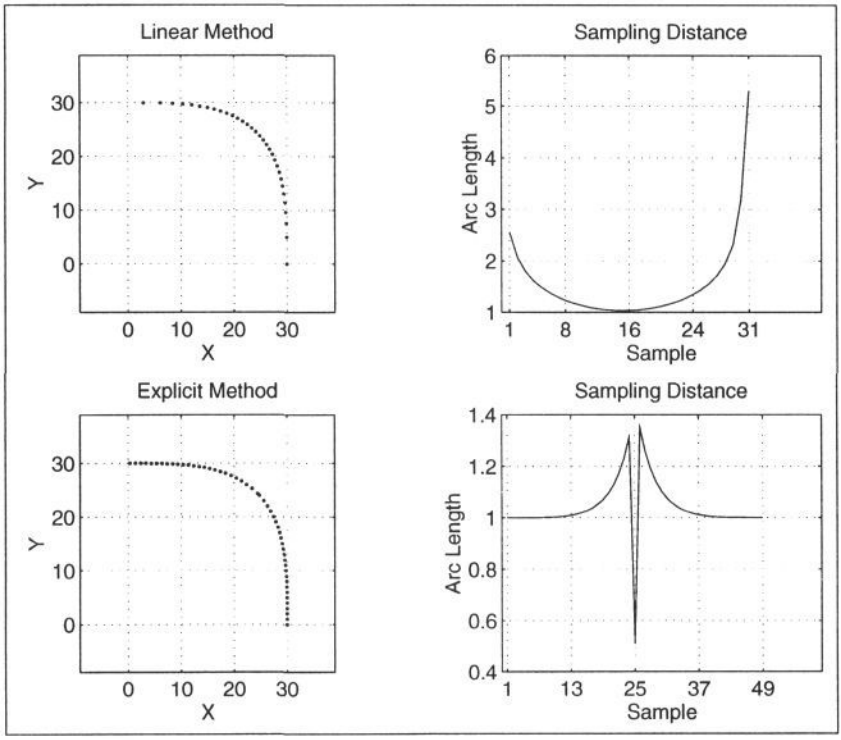

Figure 2: Example of Linear Sampling (top) and Explicit Method (bottom) with respective sampling distances

4 Optimal Parametric Sampling

In order to avoid the high discrepancy of sampling distance on the superellipse contour, we can employ a simple first-order differential model which will allow sampling to be done according to local curvature properties.

4.1 First model

Consider the parametric equation of a superellipse (1). We can approximate the arclength between two close points $\mathbf{x}(\theta)$ and $\mathbf{x}(\theta + \Delta_\theta(\theta))$ by the segment linking the two points:

$$\mathbf{D}(\theta)^2 = |\mathbf{x}(\theta + \Delta_\theta(\theta)) - \mathbf{x}(\theta)|^2$$

Assuming relatively small $\Delta_\theta(\theta)$, the right hand side of this equation can be approximated to first order by:

$$\mathbf{D}(\theta)^2 = \left(\frac{\partial}{\partial\theta}(a_1 cos(\theta)^\epsilon)\Delta_\theta(\theta)\right)^2 + \left(\frac{\partial}{\partial\theta}(a_2 sin(\theta)^\epsilon)\Delta_\theta(\theta)\right)^2$$

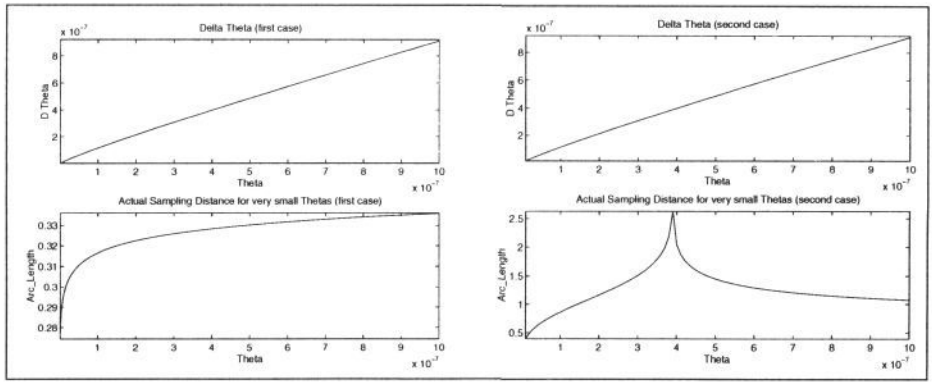

Figure 3: Actual distance for small θ

By expanding and solving this equation for Δ_θ we obtain:

$$\Delta_\theta(\theta) = \frac{\mathbf{D}(\theta)}{\epsilon}\sqrt{\frac{cos(\theta)^2 sin(\theta)^2}{a_1^2(cos(\theta)^\epsilon)^2 sin(\theta)^4 + a_2^2(sin(\theta)^\epsilon)^2 cos(\theta)^4}} \tag{5}$$

If we want to have an equal distance sampling for any θ we must set $\mathbf{D}(\theta)$ to a constant $\mathbf{K}$ that represents the approximate arclength between two sampled points; $\mathbf{D}(\theta)$ could also been adaptively changed for different kind of samplings or to cope with deformations.

The two dual updating algorithms for θ should then be as simple as:

$$\theta_i = \theta_{i-1} + \Delta_\theta(\theta_i) \qquad \theta_0 = 0\ ,\quad i \in \{1..N\} \mid \theta_N < \pi/2 \tag{6}$$

$$\theta_i = \theta_{i-1} - \Delta_\theta(\theta_i) \qquad \theta_0 = \pi/2\ ,\quad i \in \{1..N\} \mid \theta_N > 0\ , \tag{7}$$

the former going up step by step from 0 to $\pi/2$ and the latter from $\pi/2$ down to 0. Unfortunately the strong non-linearities of the superellipses cause this approximation to be wrong for θ close to 0 and $\pi/2$, and even the sampling schemes (6) and (7), apparently equivalent, have slightly different behaviour. In fact the sampling distance increases as θ increases due to the first order (linear) approximation we have used: in regions of *increasing* curvature the computed derivative overestimates the rate of change in θ needed to obtain a certain arclength whereas in regions of *decreasing* curvature the exact opposite happens. As a result the real arclength is much lower that it should be in some regions and much higher in others. Figure 3 highlights this effect for very small θ (in which the rate of change in the curvature tends to infinity) in the case of sampling scheme (6) (on the left) and (7) (on the right). (It should be noticed that the second case (right) is equivalent to sampling with scheme (6) used near $\pi/2$.) In the first case θ goes to zero very quickly whereas in the second it tends to infinity but once $\theta - \Delta_\theta$ goes below zero, its behaviour inverts and becomes similar to the one in the first case.

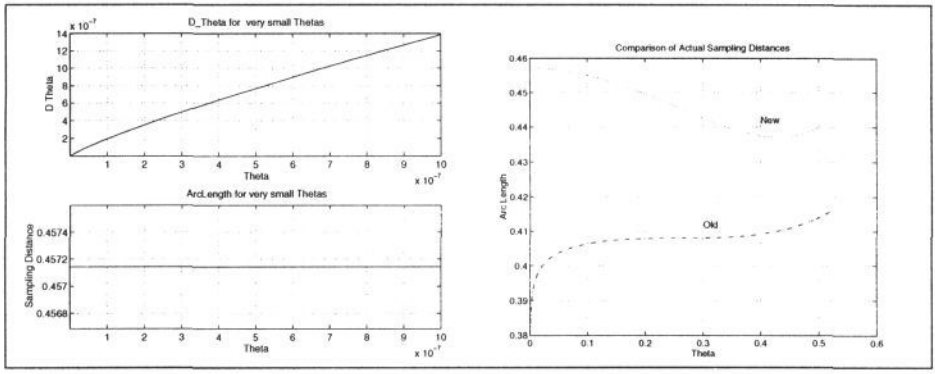

Figure 4: New approximation for small θ (left) and a comparison to the previous method for larger θ (right)

4.2 Singularities

To avoid problems at the singularities, we found that the following simple model yields a very good approximation to the equal-distance sampling near the singularities $\theta = 0$ and $\theta = \pi/2$.

In the case with $\theta \to 0$, equation (5) can be approximated as:

$$\mathbf{x}(\theta) = \begin{bmatrix} a_1 \\ a_2\theta^\epsilon \end{bmatrix}$$

and hence the distance between two points in this case is therefore:

$$\mathbf{D}(\theta) = y(\theta + \Delta_\theta(\theta)) - y(\theta) = a_2(\theta + \Delta_\theta(\theta))^\epsilon - a_2\theta^\epsilon$$

By solving for $\Delta_\theta(\theta)$ we obtain:

$$\Delta_\theta(\theta) = \left(\frac{\mathbf{D}(\theta)}{a_2} - \theta^\epsilon\right)^{\frac{1}{\epsilon}} - \theta \tag{8}$$

Analogously, for $\theta \to \pi/2$ we have:

$$\Delta_\theta(\theta) = \left(\frac{\mathbf{D}(\theta)}{a_1} - (\pi/2 - \theta)^\epsilon\right)^{\frac{1}{\epsilon}} - (\pi/2 - \theta) \tag{9}$$

with $\mathbf{D}(\theta)$ set to a constant $\mathbf{K}$ if we want equal-distance sampling.

Figure 4 shows how this new model behaves for very small θs; again we have $\epsilon = 0.1$, $a_1 = 20$, $a_2 = 20$. A quick comparison with Figure 3 shows that the actual distance with this new sampling model is practically constant with θ, which is what we wanted to achieve. For larger values of θ, as expected, this approximation does not hold any longer and some small errors are introduced. It should be noticed, however, that here we have used a low value of roundness ($\epsilon = 0.1$) and this is why the small-θ approximation holds even for relatively large values of θ. For rounder

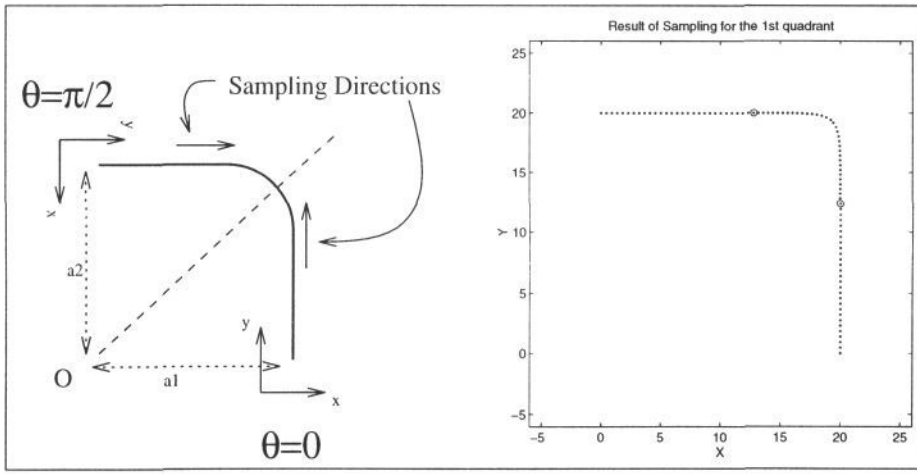

Figure 5: Swapping of axes (left) and final sampling result

shape this approximation will hold for smaller and smaller values of θ but, at the same time, the distance Equation (6) will become more and more suitable because the non-linearities becomes less strong.

4.3 Combination of the Two Models

Let *Model A* be the model of Section 4.1 and *Model B* be the one of Section 4.2 which is to be used near the singularities $\theta = 0$ and $\theta = \pi/2$.

We switch between the two models after θ and $\pi/2 - \theta$ go below a certain threshold τ. Experimentally, we have found that a good value of τ is 10^{-2}, which gives relatively smooth change in the actual sampling distance both for very small and large ϵ.

When (9) is used, however, there is a problem caused by the subtraction $(\pi/2 - \theta)$ since the numerical precision necessary to use (9) for small values of ϵ is very high. We solved this problem by swapping the x and y axis in the superellipse equation (1) in order to have the condition $\theta \to 0$ in place of $\theta \to \pi/2$; a_1 will be then used instead of a_2 in order to have exactly the same shape, as shown in Figure 5 (left).

Figure 5 (right) shows the result of this sampling method ($\epsilon = 0.1$), where the small circles indicates the swapping points between Model A and Model B; note that in this example the position of these two circles represent a distance in the parameter space θ of just $\tau = 10^{-2}$ radians!)

Figure 6 gives another full example in which θ, Δ_θ, the actual distance $D(\theta)$ and the sampled superellipse are given for $\epsilon = 0.2$, $a_1 = 20$, $a_2 = 20$. The discontinuities at **A** and **B** are due to the swap from model A and model B and the steep spike at **C** is caused by an unavoidable mismatch of the two halves of sampling joined together as shown in Figure 5. In both example it can be seen how good is the sampling, with an error in the actual distance as low as 5% on

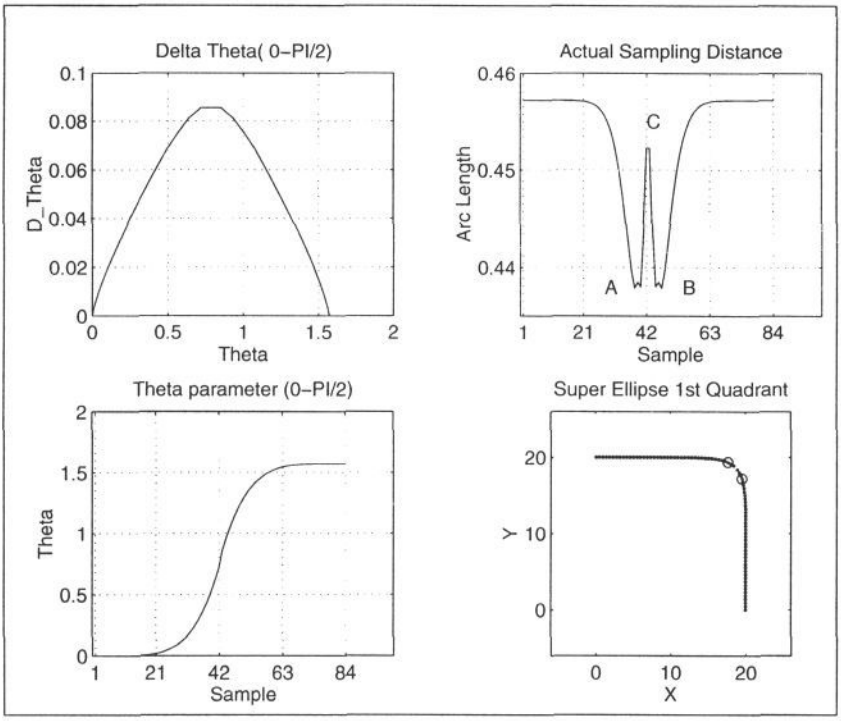

Figure 6: Two examples of equal-distance sampling (see text)

the full $[0..\pi/2]$ range.

The full sampling of the superellipse contour for $\theta = [-\pi..\pi]$ is trivially obtained by mirroring and reversing the first quadrant.

5 Extension to Deformed Superellipses

Superellipses are of particular utility when deformed because they can represent more complex shapes. When any deformations, such as tapering and bending, are applied the sampling distance changes along the contour; Figure 7 (top) shows this effect for the first quadrant of a tapered superellipse ($\epsilon = 0.5$, $T_x = 0.7$ and $\mathbf{K} = 3$) sampled with the Frankin and Barr's method [2] with the corresponding sampling distance. As it can be seen the error is rather big.

We show now how to extend the proposed method for tapered superellipses. (The same idea could be employed to deal with bending deformations but with more complex formulae).

By combining (1) and (3), the equation of a linearly tapered superellipse can be written as:

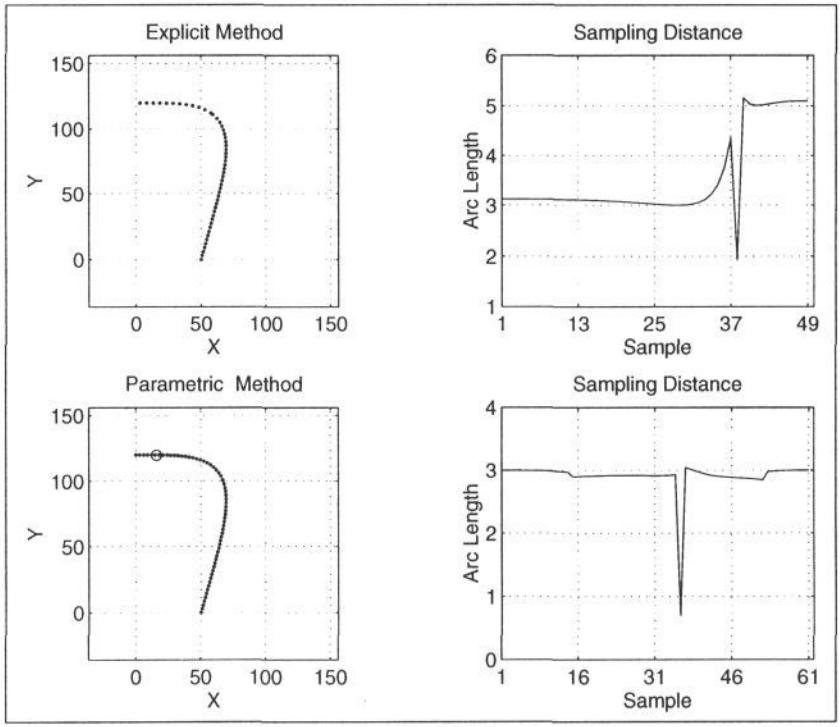

Figure 7: Example of sampling a deformed superellipse: explicit method (top) and proposed parametric method (bottom)

$$\begin{cases} x(\theta) = (T_x sin(\theta)^\epsilon + 1) a_1 cos(\theta)^\epsilon \\ y(\theta) = a_2 sin(\theta)^\epsilon \end{cases}$$

As in Section 4.1, we can express the sampling distance $\mathbf{D}(\theta)$ as a function of $\mathbf{\Delta}_\theta(\theta)$ and by solving for the latter we have:

$$\mathbf{\Delta}_\theta(\theta) = \mathbf{D}(\theta) \sqrt{\left(\frac{\partial x(\theta)}{\partial \theta}\right)^2 + \left(\frac{\partial y(\theta)}{\partial \theta}\right)^2}$$

Near the singularities we need to employ a different model and we used the same as Section 4.2 but with a modified sampled distance **K'** instead of **K** to take into account what the distance will be *after* the deformation. By considering the tapering geometry and assuming that near the singularities the shape is practically straight, we have:

$$\begin{cases} \theta \to 0: & \mathbf{K}' = \mathbf{K} atan\left(\frac{a_1 T_x}{a_2}\right) \\ \theta \to \pi/2: & \mathbf{K}' = \mathbf{K} \frac{1}{T_x + 1} \end{cases}$$

Figure 7 (bottom) shows the result of this sampling method in the same case as before along with the actual sampling distance; from the latter graph it can be seen that the improvement has been significant in all the $[0..\pi/2]$ range.

6 Discussion

Superellipses are useful parametric models for representing two dimensional object parts or aspects of 3-D parts.

In this work we have presented a parametric method that is able to achieve equal-distance sampling of superellipse models contours and that can also cope with deformations, whereas previous methods were unprecise and usable only with undeformed models. The method can also be simply extended to superquadrics using a spherical product of two superellipses.

We are currently investigating using deformable superellipses as primitives for interpreting static 2-D images of natural 3-D objects under the new framework of Model-based Optimisation, in which data segmentation and fitting is done in single unified process. In this context, a proper cumulative cost function is computed along the contour instances and a precise sampling allows all contour parts to have the same weights in final result, improving accuracy and stability of the solutions.

References

[1] A. Barr. Superquadrics and angle preserving transformations. *IEEE Computer Graphics Applications*, 1:1–20, 1981.

[2] W. Franklin and A. Barr. Faster calculation of superquadric shapes. *IEEE Computer Graphics and Applications*, July 1981.

[3] M. Gardiner. The superellipse: a curve that lies between the ellipse and the rectangle. *Scientific American*, Sept. 1965.

[4] A. Pentland. Perceptual organization and the representation of natural form. *Artificial Intelligence*, 28:293–331, 1986.

[5] A. Pentland and S. Scarloff. Closed-form solutions for physically based shape modelling and recognition. *IEEE PAMI*, 13(7), July 1991.

[6] M. Pilu and R. Fisher. Representation of 3-D part aspects by deformable superellipses. Technical report, Department of Artificial Intelligence, University of Edinburgh, 1995. In Preparation.

[7] N. Raja and A. Jain. Recognizing geons from superquadrics fitted to range data. *Image and Vision Computing*, 12(3):179–189, Apr. 1992.

[8] K. Wu and M. Levine. Recovering of parametric geons from multiview range data. In *IEEE Conference on Computer Vision and Pattern Recognition*, Seattle, WA, 1994.